Diffusion processes in single-atom electromigration along a gold chain: First-principles calculations

Masaaki Araidai[1,2,3,*] and Masaru Tsukada[1,3,4,†]

[1]*WPI Advanced Institute for Materials Research, Tohoku University, 2-1-1 Katahira, Aoba-ku, Sendai, Miyagi 980-8577, Japan*

[2]*Institute for Nanoscience and Nanotechnology, Waseda University, Japan*

[3]*CREST, Japan Science and Technology Agency*

[4]*Department of Nanoscience and Nanoengineering, Waseda University, Japan*

(Received 7 May 2009; revised manuscript received 15 June 2009; published 16 July 2009)

Electromigration of a single atom along a chain of gold atoms was investigated by first-principles calculations based on the nonequilibrium Green's-function technique combined with density-functional theory. In the case of electromigration of a gold atom, we found that the potential barrier along the migration pathway decreases as the applied bias voltage is increased and the migration direction is the same as that of electron flow. By considering the case of electromigration of a sulfur atom along the gold chain, we determined that the electron flow around the migrating atom is responsible for single-atom electromigration. The calculated electromigration rate for the gold atom indicated that the electromigration takes place at temperatures above room temperature.

DOI: 10.1103/PhysRevB.80.045417 PACS number(s): 66.30.Qa, 73.40.Jn, 73.63.−b

I. INTRODUCTION

Flow of electrons in electrical conductors can lead to drastic rearrangement and diffusion of atoms owing to current-induced forces, resulting in the failure of interconnects in integrated circuits. This so-called electromigration is a key issue, especially for nanoscale conductors with much larger current densities than their macroscopic counterparts.

The theoretical study of electromigration has a long history.[1] Traditionally, the microscopic origin of the current-induced force on an atom has been discussed in terms of electrostatic forces and momentum transfer by the electron flow (electron wind force). However, such a division depends on analytical approaches and leaves certain issues somewhat ambiguous. On the other hand, in recent computational studies of open systems under nonequilibrium conditions, the current-induced force in nanoscale conductors has been calculated without making such a division. Di Ventra and co-workers discussed the origin of the forces[2–4] and investigated the stability of carbon-based molecular junctions against electric currents.[5] They calculated the so-called Hellmann-Feynman force that includes both the electrostatic and wind forces within the elastic-transport regime using the adiabatic approximation.[2,6] Brandbyge *et al.*[7] described how a small gold chain would be distorted by an applied current while Mingo *et al.*[8] investigated the forces experienced by ions in the vicinity of conducting carbon nanotubes. These studies focused on how the current modifies the bonding strength between the atoms. On the other hand, only a few theoretical studies have been devoted to the investigation of atomic-diffusion processes during electromigration.[9]

From an experimental point of view, electromigration has recently been put to practical use in fabricating metallic electrodes with a nanosized gap between them.[10–17] Such nanogap electrodes can be used in various areas of nanotechnology such as a fabrication of single molecular devices in which an organic molecule is sandwiched between the electrodes.[18–21] More recently, in the fabrication of nanogap electrodes by the electromigrated break-junction technique, Umeno and Hirakawa[22] have observed an intriguing stepwise decrease over time of the electrical conductance of gold junctions. This behavior resulted from the disappearance of a conducting channel (6*s* orbital) of a gold atom at the junction and implied that the electromigration of *single* gold atoms takes place steadily at a threshold voltage (0.3–0.4 V). Motivated by this experiment, in this study, we investigate single-atom electromigration as one of the elementary processes in nanogap formation using first-principles calculations.

The outline of this paper is as follows. The computational method and model used here are described in Sec. II. In Sec. III, we present numerical results for the electromigration of a single gold atom along a straight one-dimensional chain of gold atoms. The bias dependence of the migration barrier heights and the migration direction are discussed together with the results for the electromigration of a single sulfur atom. We also calculate the electromigration rate in order to theoretically predict the temperature around the migrating gold atom. Section IV is devoted to a summary of this paper.

II. METHOD AND MODEL

We employed the nonequilibrium Green's-function technique combined with density-functional theory[23] (NEGF+DFT) which has been developed for the numerical analysis of open systems under nonequilibrium conditions.[24,25] The premise of this method is to divide the system into three regions: the left and right electrodes in thermal equilibrium and the central scattering region in which nonequilibrium electron densities are self-consistently calculated. The Green's function of the scattering region includes the self-energy generated by the electrodes through a self-consistent DFT scheme. As the Kohn-Sham Hamiltonian $\hat{H}$ and the associated density matrix $\hat{D}$ are determined by the NEGF+DFT technique, the force acting on the ith atom $\boldsymbol{F}_i$ is

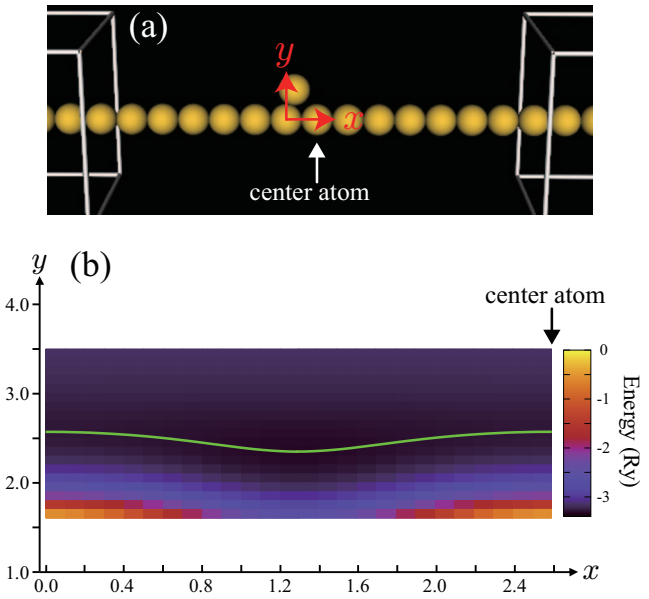

FIG. 1. (Color) (a) Calculation model for single-atom electromigration along a gold atomic chain. White boxes denote the electrode regions. A single gold or sulfur atom migrates along the chain. (b) PES for the migrating atom. (The PES shown here is the case for a gold atom at zero bias.) The x and y axes are defined in (a) and expressed in units of Å. The green line indicates the migration pathway, that is, determined as a valley of the PES.

readily given by the Hellmann-Feynman theorem[7]

$$\boldsymbol{F}_i = \mathrm{Tr}[\hat{F}_i \hat{D}] - \frac{\partial \hat{H}_{ii}}{\partial \boldsymbol{R}_i} \quad \text{with} \quad \hat{F}_i = -\frac{\partial \hat{H}}{\partial \boldsymbol{R}_i}, \tag{1}$$

where $\hat{F}_i$ is the force operator with respect to the ith atom ($\boldsymbol{R}_i$) and $\hat{H}_{ii}$ is the interaction between atoms. We used the commercially available Atomistix ToolKit (ATK).[26] This code employs numerical atomic orbitals and norm-conserving pseudopotentials.[27]

In the present study, the left and right electrodes are semi-infinite gold chains and the scattering region is a portion of the chain with 14 gold atoms and a single adatom (gold or sulfur) that migrates along the chain, as shown in Fig. 1(a). Although the stable structure of a chain of gold atoms has been found from DFT calculations to have a zigzag shape,[28] we adopted a straight chain for simplicity. The bond length between the gold atoms in the chain was fixed at 2.5875 Å, which was evaluated from DFT calculations under periodic boundary conditions using the ATK. We used double-zeta orbitals with polarization and the local-density approximation for the exchange-correlation potential.[29] The cutoff energy was 150 Ry.

The procedure of the theoretical analysis is as follows. First, we calculate the forces acting on the migrating atom under bias voltages. Next, potential-energy surfaces (PESs) for the migrating atom are evaluated from the relation between force and potential energy $U(\boldsymbol{r})$,

$$U(\boldsymbol{r}) = -\int_C \boldsymbol{F}(\boldsymbol{s}) \cdot d\boldsymbol{s}, \tag{2}$$

where C is an integration route. Although the total energy is not precisely defined for an open system, the potential energy can be calculated by Eq. (2). Recently, the nonconservative character of the current-induced force has been reported in molecular-dynamics simulations.[30] If the current-induced force is not conservative, then the potential energy cannot be safely associated to them. However, our analysis by the PES is reasonable because in our situation the above integral was *not* path dependent within the calculation accuracy, namely, the calculated force is conservative. The PES for the gold atom at a bias of 0 V is given in Fig. 1(b). From these PESs, we can estimate the migration pathway indicated by a green solid line in Fig. 1(b) and also obtain some valuable information concerning the electromigration mechanism.

III. RESULTS AND DISCUSSION

A. Bias dependence of electromigration barrier and the migration direction

Figure 2(a) shows potential-energy curves for a gold atom that migrates around the center of the chain. The horizontal

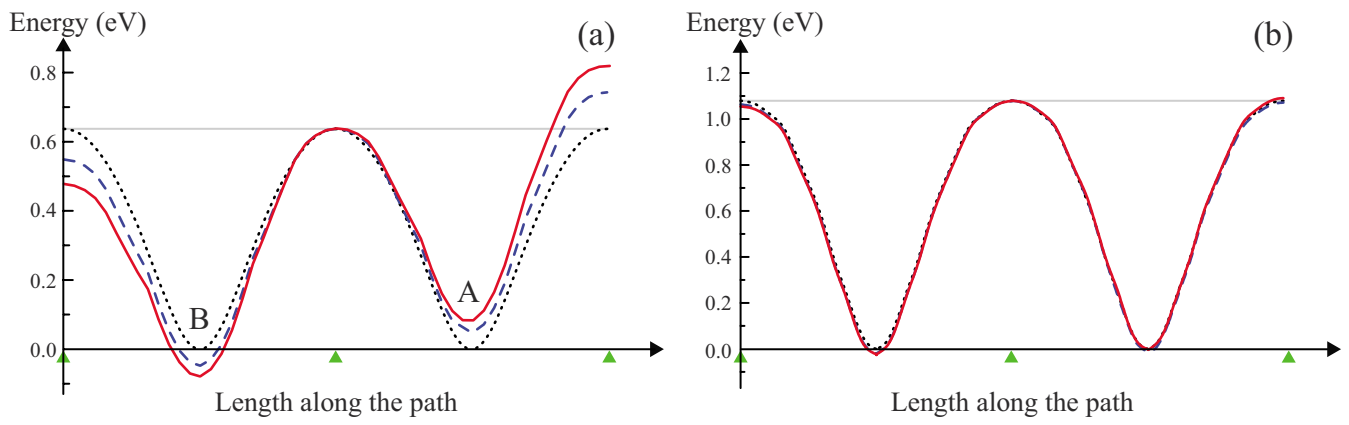

FIG. 2. (Color online) Potential-energy curves along the migration pathways for (a) gold and (b) sulfur atoms at 0.0 (dotted black), 0.1 (dashed blue), and 0.2 (solid red) V. [The migration pathway at zero bias is depicted as the green line in Fig. 1(b).] Green triangles indicate atomic positions of the gold atoms in the chain projected onto the pathway. The central triangle is the center of the chain.

TABLE I. The barrier height (eV) for electromigration for a gold atom at each bias voltage (V). A and B are defined as local minima of the potential-energy curves close to the center of the chain, as shown in Fig. 2(a).

Bias	0.0	0.1	0.2
$A \rightarrow B$	0.64	0.59	0.56
$B \rightarrow A$	0.64	0.68	0.71

axis corresponds to the length along the migration pathway determined as a valley in the PES. [See Fig. 1(b) for the pathway at zero bias.] The dotted black, dashed blue, and solid red curves denote the results for biases of 0.0, 0.1, and 0.2 V, respectively. The green triangles indicate the positions of the chain atoms which are projected onto the pathway. The local minima of the potential-energy curves, depicted by A and B in Fig. 2(a), correspond to the stable positions at which the migrating atom forms a triangle with two gold atoms in the chain. This result is reasonable considering that the stable surface structure of gold is the (111) surface with a triangular lattice.

We immediately observe in Fig. 2(a) that the potential barrier for electromigration decreases steadily with an increase in applied bias voltage. The values of the migration barrier heights are listed in Table I. It is found from Fig. 2(a) and Table I that the bias dependence of the barrier reduction ($A \rightarrow B$) deviates slightly from a linear relation. A similar nonlinear relation between the bias and current-induced force has been reported by Yang and Di Ventra.[3] The most important observation from Fig. 2(a) is that the potential curves show a downward trend toward the left side of the graph. Note that the bias voltage V_{bias} is related to the difference between the Fermi energies of the left and right electrodes. In the present case, the Fermi energy of the right electrode is eV_{bias} higher than that of the left electrode, meaning that electrons flow from the right to left electrodes. This means that the gold atom migrates in the same direction as the electron flow. This result has been confirmed by recent experimental observations.[31]

If the contribution of the external electric field to the electromigration is distinguished from the contribution of electric current as in the traditional theory of electromigration, then in the present situation the electric-field contribution is opposite to the direction of electron flow because the gold atom is always positively charged on the migration pathway [$+0.19e$ at the local minimum A in Fig. 2(a)]. Thus, considering that the overall appearance of the potential curves in Fig. 2(a), we find that the contribution of the electric current is dominant in the electromigration of the gold atom.

In order to verify that the electron flow is responsible for the electromigration, we also performed calculations for the electromigration of a single sulfur atom along the same chain. The $3p$ orbitals of the sulfur atom hybridized with $5d$ orbitals of the gold atom have a much lower energy than the Fermi level. Therefore, it is expected that for electromigration of the sulfur atom the electric-current contribution would be small due to the absence of electrons around the bias window. Figure 2(b) shows the potential-energy curves

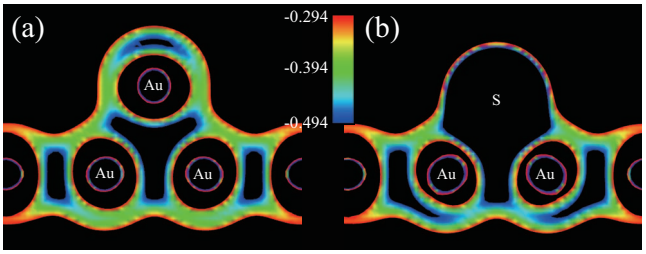

FIG. 3. (Color) The effective potentials around the migrating (a) gold and (b) sulfur atom at a bias of 0.2 V. In both cases, the migrating atom is placed at the position of the local minimum which appears on the right side in Figs. 2(a) and 2(b). The range of the contour corresponds to the bias window. The value −0.394 eV in the color bar is the averaged Fermi energy of the left and right electrodes.

along the migration pathway of the sulfur atom. Obviously, the bias dependence is negligibly small. To clarify the contribution of the electron flow, the effective electron potentials $V_{\mathrm{eff}}(\boldsymbol{r})$ around the migrating atom at a bias of 0.2 V are given in Fig. 3. $V_{\mathrm{eff}}(\boldsymbol{r})$ within the bias window indicates the path through which electrons flow. In the case of sulfur [Fig. 3(b)], the current path is very narrow around the sulfur atom, leading to a small contribution from the electric current, as predicted above. On the other hand, the current path around the gold atom is much wider, as seen in Fig. 3(a). It seems reasonable from the distribution of $V_{\mathrm{eff}}(\boldsymbol{r})$ that the electron flow around the migrating atom is responsible for single-atom electromigration.

B. Electromigration rate

We previous showed that the electromigration barrier for a gold atom steadily decreases as the applied voltage increases. However, the barrier remains high enough to prevent the gold atom from migrating along the chain. It is expected that this barrier is overcome by the thermal energy associated with Joule heating. Accordingly, we next estimate the electromigration rate as a function of the temperature.

The migration rate Γ is obtained from the below equation,

$$\Gamma = \nu \exp(-E/k_{\mathrm{B}}T), \tag{3}$$

where ν, E, k_{B}, and T are the attempt frequency, potential-barrier height, Boltzmann constant, and temperature, respectively. In this case, we have two events 1 and 2 as defined in the schematic diagram shown in Fig. 4. The barrier heights for the events, E_1 and E_2, are readily evaluated from the PES given in Fig. 2(a) as $E_1=0.56$ eV and $E_2=0.74$ eV. The attempt frequencies, ν_1 and ν_2, obtained by fitting a quadratic function to the local minimum of the potential-energy curve as shown by the dashed curve in Fig. 4 are $\nu_1=\nu_2=2.13$ THz. T is also treated as a parameter.

The values of Γ as a function of T are listed in Table II. An exponential increase in both Γ and migration velocity with increasing temperature can be clearly seen. Migration rates of more than one per second have already been experimentally observed.[22,31] Taking these observations into account, we can predict from the theoretical calculations that

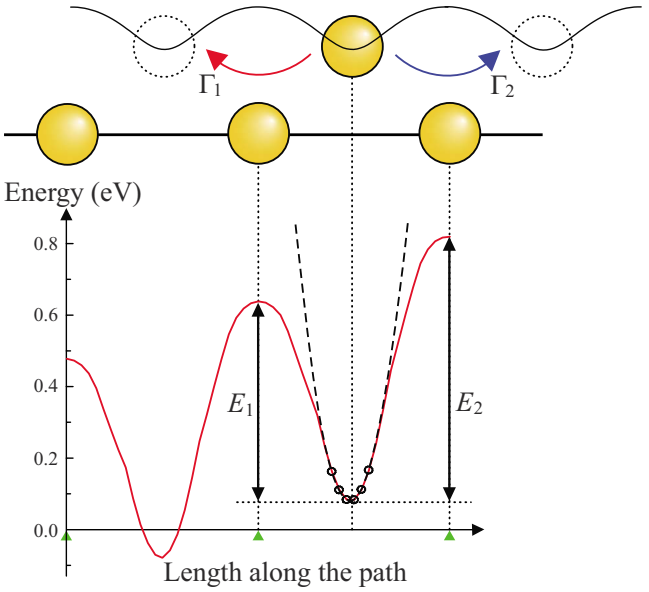

FIG. 4. (Color online) Potential-energy curve along the migration pathway for a gold atom at a bias of 0.2 V, together with the atomic configurations during the migration events. The parabola indicated by the dashed curve denotes the fitting curve used to estimate the spring constant.

the single-atom electromigration takes place at temperatures higher than room temperature.

IV. SUMMARY

Single-atom electromigration along a chain of gold atoms was investigated by first-principles calculations based on NEGF+DFT. We found from the potential energy along the migration pathway that the applied voltage steadily reduces the potential barrier for electromigration. The gradient of the potential curves indicates that the gold atom migrates in the same direction as the electron flow. This has recently been confirmed experimentally in gold junction systems. By comparing electromigration of gold and sulfur atoms, we verified that electron flow around the migrating atom is responsible for single-atom electromigration. We also calculated the electromigration rate to theoretically estimate the temperature around the migrating gold atom. The results showed that single-atom electromigration takes place at temperatures higher than room temperature.

TABLE II. Electromigration rates (1/s) for each temperature (K). The events 1 and 2 are defined in Fig. 4. The migration velocities V for event 1 are also listed.

T	Γ_1	Γ_2	V
100	1.30×10^{-16}	1.11×10^{-25}	3.36×10^{-16} Å/s
300	8.34×10^{2}	7.96×10^{-1}	215.80 nm/s
500	4.84×10^{6}	7.45×10^{4}	125.24 μm/s

ACKNOWLEDGMENTS

The authors thank Akinori Umeno and Kazuhiko Hirakawa for their intriguing experiments and fruitful discussions, and also Yoshifumi Oshima for valuable discussions on electromigration in gold junction systems. The computation of this work was performed in part at the Supercomputer Center, Institute for Solid State Physics, University of Tokyo. This research was supported by a Grant-in-Aid for Scientific Research on Priority Areas "Electron transport through a linked molecule in nanoscale" from the Ministry of Education, Culture, Sports, Science and Technology of Japan.

*araidai@wpi-aimr.tohoku.ac.jp
†tsukada@wpi-aimr.tohoku.ac.jp

[1] R. S. Sorbello, Solid State Phys. **51**, 159 (1997), and references therein.
[2] M. Di Ventra and S. T. Pantelides, Phys. Rev. B **61**, 16207 (2000).
[3] Z. Yang and M. Di Ventra, Phys. Rev. B **67**, 161311(R) (2003).
[4] M. Di Ventra, Y.-C. Chen, and T. N. Todorov, Phys. Rev. Lett. **92**, 176803 (2004).
[5] M. Di Ventra, S. T. Pantelides, and N. D. Lang, Phys. Rev. Lett. **88**, 046801 (2002).
[6] T. N. Todorov, J. Hoekstra, and A. P. Sutton, Philos. Mag. B **80**, 421 (2000).
[7] M. Brandbyge, K. Stokbro, J. Taylor, J.-L. Mozos, and P. Ordejon, Phys. Rev. B **67**, 193104 (2003).
[8] N. Mingo, L. Yang, and J. Han, J. Phys. Chem. B **105**, 11142 (2001).
[9] M. Araidai and K. Watanabe, e-J. Surf. Sci. Nanotechnol. **5**, 106 (2007).
[10] H. Park, A. K. L. Lim, A. P. Alivisatos, J. Park, and P. L. McEuen, Appl. Phys. Lett. **75**, 301 (1999).
[11] D. R. Strachan, D. E. Smith, D. E. Johnston, T.-H. Park, M. J. Therien, D. A. Bonnell, and A. T. Johnson, Appl. Phys. Lett. **86**, 043109 (2005).
[12] G. Esen and M. S. Fuhrer, Appl. Phys. Lett. **87**, 263101 (2005).
[13] A. A. Houck, J. Labaziewicz, E. K. Chan, J. A. Folk, and I. L. Chuang, Nano Lett. **5**, 1685 (2005).
[14] R. Sordan, K. Balasubramanian, M. Burghard, and K. Kern, Appl. Phys. Lett. **87**, 013106 (2005).
[15] K. O'Neill, E. A. Osorio, and H. S. J. van der Zant, Appl. Phys. Lett. **90**, 133109 (2007).
[16] Z. M. Wu, M. Steinacher, R. Huber, M. Calame, S. J. van der Molen, and C. Schönenberger, Appl. Phys. Lett. **91**, 053118 (2007).
[17] M. Tsutsui, M. Taniguchi, and T. Kawai, Appl. Phys. Lett. **93**, 163115 (2008).
[18] H. Park, J. Park, A. K. L. Lim, E. H. Anderson, A. P. Alivisatos, and P. L. McEuen, Nature (London) **407**, 57 (2000).
[19] J. Park, A. N. Pasupathy, J. I. Goldsmith, C. Chang, Y. Yaish, J. R. Petta, M. Rinkoski, J. P. Sethna, H. D. Abruña, P. L. McEuen,

and D. C. Ralph, Nature (London) **417**, 722 (2002).
[20] E. A. Osorio, K. O'Neill, M. Wegewijs, N. Stuhr-Hansen, J. Paaske, T. Bjornholm, and H. S. J. van der Zant, Nano Lett. **7**, 3336 (2007).
[21] Y. Noguchi, R. Ueda, T. Kubota, T. Kamikado, S. Yokoyama, and T. Nagase, Thin Solid Films **516**, 2762 (2008).
[22] A. Umeno and K. Hirakawa, Appl. Phys. Lett. **94**, 162103 (2009).
[23] W. Kohn and L. J. Sham, Phys. Rev. **140**, A1133 (1965).
[24] J. Taylor, H. Guo, and J. Wang, Phys. Rev. B **63**, 245407 (2001).
[25] M. Brandbyge, J.-L. Mozos, P. Ordejon, J. Taylor, and K. Stokbro, Phys. Rev. B **65**, 165401 (2002).
[26] QUANTUMWISE HP, http://www.quantumwise.com/
[27] N. Troullier and J. L. Martins, Phys. Rev. B **43**, 1993 (1991).
[28] J. Nakamura, N. Kobayashi, S. Watanabe, and M. Aono, Surf. Sci. **482-485**, 1266 (2001).
[29] J. P. Perdew and A. Zunger, Phys. Rev. B **23**, 5048 (1981).
[30] M. Brandbyge, Nat. Nanotechnol. **4**, 81 (2009); D. Dundas, E. J. McEniry, and T. N. Todorov, *ibid.* **4**, 99 (2009).
[31] Y. Oshima (private communication).